Tribological Study of Friction in Roller Follower Valve Train Considering Effects of Asperity Interaction and Roller Sliding

Author

TAYYAB UL ISLAM

Regn. Number

00000206131

Supervisor

DR RIAZ AHMAD MUFTI

DEPARTMENT OF MECHANICAL ENGINEERING

SCHOOL OF MECHANICAL & MANUFACTURING ENGINEERING

NATIONAL UNIVERSITY OF SCIENCES AND TECHNOLOGY

ISLAMABAD

SEPTEMBER, 2019

Tribological Study of Friction in Roller Follower Valvetrain Considering Effects of Asperity Interaction and Roller Sliding

Author

TAYYAB UL ISLAM

Regn Number

00000206131

A thesis submitted in partial fulfillment of the requirements for the degree of

MS Mechanical Engineering

Thesis Supervisor:

DR. RIAZ AHMAD MUFTI

Thesis Supervisor's Signature: _____

DEPARTMENT OF MECHANICAL ENGINEERING

SCHOOL OF MECHANICAL & MANUFACTURING ENGINEERING

NATIONAL UNIVERSITY OF SCIENCES AND TECHNOLOGY,

ISLAMABAD

SEPTEMBER, 2019

National University of Sciences & Technology

MASTER THESIS WORK

We hereby recommend that the dissertation prepared under our supervision by: **TAYYAB UL ISLAM (00000206131)** Titled: **Tribological Study of Friction in Roller Follower Valve Train Considering Effects of Asperity Interaction and Roller Sliding** be accepted in partial fulfillment of the requirements for the award of **MS Mechanical Engineering** degree with_____ grade.

Examination Committee Members

1. Name: <u>Dr. Samiur Rahman Shah</u>   Signature:_____

2. Name: <u>Dr. Mian Ashfaq Ali</u>   Signature:_____

3. Name: <u>Dr. Rehan Zahid</u>   Signature:_____

Supervisor's name: _____   Signature:_____

Date:_____

_____   _____
Head of Department   Date

COUNTERSINGED

Date:_____   _____
                                   Dean/Principa

THESIS ACCEPTANCE CERTIFICATE

Certified that final copy of MS thesis written by Mr.**TAYYAB UL ISLAM** (Registration No.00000206131), of **School of Mechanical & Manufacturing Engineering** has been vetted by undersigned, found complete in all respects as per NUST Statutes / Regulations, is free of plagiarism, errors, and mistakes and is accepted as partial fulfillment for award of MS/MPhil degree. It is further certified that necessary amendments as pointed out by GEC members of the scholar have also been incorporated in the said thesis.

Signature: _____

Name of Supervisor: _____

Date:_____

Signature (HOD): _____

Date:_____

Signature (Dean/Principal): _____

Date:_____

Declaration

I certify that this research work titled "*Tribological Study of Friction in Roller Follower Valve Train Considering Effects of Asperity Interaction and Roller Sliding*" is my own work. The work has not been presented elsewhere for assessment. The material that has been used from other sources it has been properly acknowledged/referred.

<div align="right">

Signature of Student

TAYYAB UL ISLAM

2017-NUST-MS-Mech-00000206131

</div>

Language Correctness Certificate

This thesis has been read by an English expert and is free of typing, syntax, semantic, grammatical and spelling mistakes. Thesis is also according to the format given by the university.

Signature of Student

TAYYAB UL ISLAM

Registration Number: 00000206131

Signature of Supervisor

Plagiarism Certificate (Turnitin Report)

This thesis has been checked for Plagiarism. Turnitin report endorsed by Supervisor is attached.

Signature of Student

TAYYAB UL ISLAM

Registration Number

00000206131

Signature of Supervisor

Copyright Statement

Acknowledgements

I am thankful to my Creator Allah Subhana-Watala to have guided me throughout this work at every step and for every new thought which You setup in my mind to improve it. Indeed I could have done nothing without Your priceless help and guidance. Whosoever helped me throughout the course of my thesis, whether my parents or any other individual was Your will, so indeed none be worthy of praise but You.

I am profusely thankful to my beloved parents who raised me when I was not capable of walking and continued to support me throughout in every department of my life.

I would also like to express special thanks to my supervisor Dr. Riaz Ahmad Mufti for his help throughout my thesis and also for Tribology and Advanced courses which he has taught me. I can safely say that I haven't learned any other engineering subject in such depth than the ones which he has taught.

I would also like to pay special thanks to Dr. Muhammad Khurram for his tremendous support and cooperation. Each time I got stuck in something, he came up with the solution. Without his help I wouldn't have been able to complete my thesis. I appreciate his patience and guidance throughout the whole thesis.

I would also like to thank Muhammad Umar and Dr. Rehan Zahid for being on my thesis guidance and evaluation committee and express my special thanks to AAA for his help.

Finally, I would like to express my gratitude to all the individuals who have rendered valuable assistance to my study.

Dedicated to my exceptional parents and adored siblings, especially my younger brother "Saqib ul Islam", whose tremendous support and cooperation led me to this wonderful accomplishment.

Abstract

The performance and durability of components in engine valve train is largely governed by the friction. The valve train is often subjected to severe and transient operating conditions promoting friction, greatly. The aim of this work is to develop a comprehensive numerical approach to analyze the friction in roller follower valve train considering the effects of roller sliding, friction due to asperity interaction and friction arising from other components under different operating conditions. Simulation results predicted that the friction from asperity interaction becomes dominant at higher oil supply temperature. High magnitude of sliding friction was observed due to the rise in roller sliding by increasing the camshaft rotational frequency and lowering the lubricant oil supply temperature. The numerical approach developed in this paper is validated by already available experimental data in the form of drive torque and good conformity between the magnitude of measured and predicted results was observed.

Key Words: *Friction force, Roller slip, Asperity interaction, Drive torque*

Table of Contents

List of Figures

CHAPTER 1: INTRODUCTION

Due to increasing demand for fuel-efficient engines, high durability and strict government policies related to emissions control have pushed the tribological components under severe operating conditions. Roller follower valve train is considered as an efficient configuration in the automotive sector due to its better lubrication performance and operational reliability [1]. However, factors like roller sliding, asperity interaction, contact loading, film thickness, cam rotational frequency and temperature can increase the fiction in valve train during operation and may affect the overall performance and life of components.

1.1   Background, Scope and Motivation

To reduce frictional losses in engines is a more suitable strategy towards improved fuel economy due to its wider scope and easy implementation as compared to other measurements. A reduction in valve train friction can also contribute to improving the overall engine efficiency as valve train friction is 10% of total engine friction at high RPM and can increase up to three folds at lower engine RPM [2]. Roller follower valve train has already proved its efficiency in terms of friction when compared to direct action valve train due to considerable reduction of sliding friction at cam follower interface [1, 3]. Quantitative insight into the friction of engine valve train can lead to advancements in cam profile design, valve timing, material for mating surfaces, lubricant formulation and characterization.

Therefore, a comprehensive understanding of frictional behavior in roller follower valve train becomes essential thereby allowing to control the factors promoting friction and improve performance.

It has been reported in the previous studies that the coefficient of friction drops to 0.003-0.006 from 0.11-0.14 by replacing the flat pad follower with a roller follower [3]. In early attempts for tribological analysis of roller follower valve train, the no-slip condition was

assumed i.e. follower bearing resistance was neglected and it was assumed that roller and cam have the same surface velocities [4-6] which reduced the accuracy of developed models. Theoretical models [7, 8] were developed after taking roller slip into account without considering the effects of asperities interactions which becomes critical at high operating temperature. The asperity interaction plays a fundamental role when the film thickness is less than the composite surface roughness heights. In the highly loaded region, the friction is governed by the asperity contact as well as tractive friction in the hydrodynamic region [9]. Khurram et al. [10] measured the average roller slip experimentally and proved its dependency on lubricant chemistry and engine operating conditions. Turturro et al. [11] have included the friction due to asperity contact in the assessment of friction but they assumed pure rolling condition at cam/roller interface. Shivam el al. [12] accounts for the roller sliding at the cam/roller interface but did not take into account the friction due to asperity contact. The contribution in the valve train friction force from the cam bearings, valve-guide interface and needle roller bearing has never been reported in the past. Moreover, the effects of the different camshaft speeds and oil supply temperature on friction in roller follower valve train were also not reported, earlier.

In this research work, a new and comprehensive numerical approach has been presented to investigate the friction in advanced end pivoted roller finger-follower valve train considering the friction due to asperity contact and roller sliding. The effects of camshaft rotational frequency and lubricant bulk temperature on friction have been analyzed in detail. The friction force from the cam bearings, valve/guide interface and needle roller bearing have also been considered to make the model more complete thereby predicting accurate drive torque. This new approach will also allow understanding of the friction mechanism in roller follower valve train comprehensively, therefore, saving time and expensive full-scale tests.

The result obtained through simulations are validated by the experimental findings presented by Abdullah et al. [13]. The experimental results are in the form of drive torque composed of geometric torque and frictional torque, therefore, friction forces of cam/roller contact and all other associated components are converted in drive torque. Good conformity in magnitude of experimental and predicted results was found.
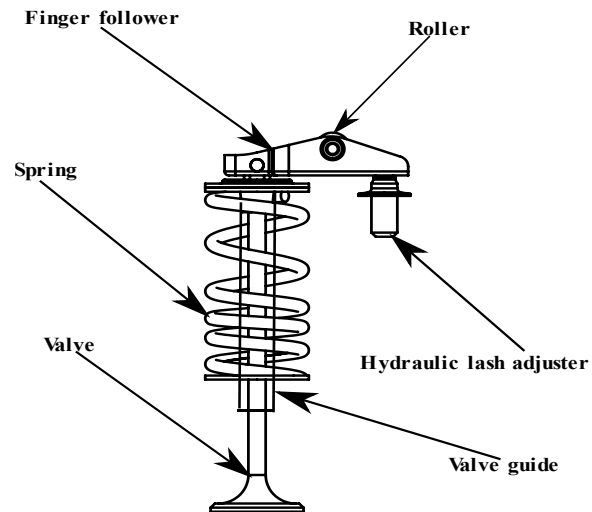
Fig. 1. Schematic of End pivoted roller finger roller follower valve train

CHAPTER 2: ANALYTICAL MODELS AND NUMERICAL METHODOLOGY

The geometry of the cam/roller follower system is shown in Fig. 2.
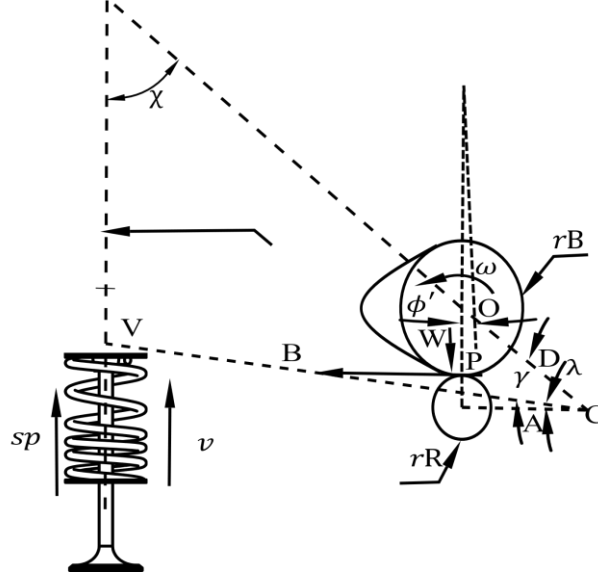
Fig. 2. Basic geometry of End pivoted roller finger-follower valve train

2.1 Kinematic Analysis

The kinematic model used here for the calculation of the equivalent radius of curvature and cam surface velocity is given by Dyson [14] and Lim et al. [15]. The general procedure can work for a different type of valve train geometries and only main equations are given here. The local radius of curvature of cam profile is given as

$$R_c = \frac{M^3}{L^2} - r_R \tag{1}$$

M and L and related variables are given as

$$L^2 = A^2(1 + \frac{d\gamma}{d\phi'})^3 - AD\frac{d^2\gamma}{d(\phi')^2}\sin(\gamma + \lambda) + D^2 - AD(1 + \frac{d\gamma}{d\phi'})(2 + \frac{d\gamma}{d\phi'}) \tag{2}$$

$$M^2 = A^2(1 + \frac{d\gamma}{d\phi'})^2 - 2AD\left(1 + \frac{d\gamma}{d\phi'}\right)\cos(\gamma + \lambda) + D^2 \tag{3}$$

$$\frac{d\gamma}{d\phi'} = [B\sin(\gamma + \chi)^{-1}](\frac{dl_v}{d\phi'}) \tag{4}$$

$$\frac{d^2\gamma}{d(\phi')^2} = [Bsin(\gamma + \chi)^{-1}]\frac{d^2l_v}{d(\phi'^2)} - [B^2sin^3(\gamma + \chi)]^{-1}(\frac{dl_v}{d\phi'})^2 cos(\gamma + \chi)) \qquad (5)$$

$$l_v = Bcos(\gamma_B + \chi) - Bcos(\gamma + \chi) \qquad (6)$$

L^2 can be less than zero its notation represent its dimension that is square of the length. Angle λ, χ and distance CR=A, CO=D, CV=B are fixed and their values are usually provided by engine manufacturers. Angle $\phi' = \theta + \phi'_0$ where θ is the angle of the camshaft, zero angle refers to the maximum lift position of cam, and ϕ'_0 is given in equation [7]. Subscript B with γ_B in equation [6] refers to its value at the base circle and given in equation [8].

$$\tan(\phi'_0) = \cot(\gamma_0 + \lambda) - \frac{D}{A}cosec(\gamma_0 + \lambda) \qquad (7)$$

$$\cos(\gamma_B + \lambda) = \frac{A^2 + D^2 - (r_R + r_B)^2}{2AD} \qquad (8)$$

γ_0 represents angle γ at the maximum lift and its value is obtained from the following relation.

$$\cos(\gamma_0 + \chi) = \cos(r_R + \chi) - \frac{l_{vo}}{B} \qquad (9)$$

where l_{vo} is lift at zero cam angle. The equivalent radius of curvature at cam follower contact point is given as

$$R = r_R - \frac{r_R L^2}{M^3} \qquad (10)$$

Consequently, the surface velocity of the contact point relative to cam is given by

$$V_c = \left(M - \frac{r_R L^2}{M^2}\right)\omega \qquad (11)$$

The work of F Ji [8] has been used to calculate the roller surface velocity with respect to the contact point. The torque balance around roller bearing is governed by torque acting at cam roller and roller pin contact, roller inertia also plays its role in computing roller surface velocity V_f given as:

$$\alpha_r = \frac{\mu W r_R - \mu_p W r_p}{I} \tag{12}$$

$$V_f(i + 1) = V_f(i) + \alpha_r \Delta t \tag{13}$$

After determining the above variables, the sliding and entrainment velocities can be calculated by given expressions.

μ_r is the coefficient of friction for the needle roller bearing. r_p is the distance from roller bearing center to pitch circle of needles given as $r_p = r_R - r_{Ri} - r_N$, Δt is time for the unit rotation of cam and $I = 0.5 M_r (r_R{}^2 + (r_{R-r_{Ri}})^2$. After determining all the above variables the sliding and entrainment velocities can be calculated.

$$V_s = V_c - V_f \tag{14}$$

$$V_e = \frac{V_c + V_f}{2} \tag{15}$$

2.2   Dynamic Analysis

The principle forces that govern the valve operation are spring force, the inertia of moving parts, friction force between moving parts, forces because of dynamic response and components damping behavior. The work of Ball [16] is referred for estimating the loading of cam/roller interface. In order to simplify the analysis, some reasonable assumptions are made while conserving the desired accuracy. The system is rigid therefore dynamic response of the valve train can be neglected, normal load on cam is slightly affected by the intercomponent friction of valve train it can also be ignored, the mass of valve, valve cap, retainer, roller pin, and spring all are referred to as single reciprocating mass, one-third of spring-mass is taken as its effective mass in calculation of normal force. The total normal load on cam is given by.

$$W = \frac{M_{sp} + M_{rf} + M_v}{A \sin(\pi - \gamma - \lambda - \chi)} \tag{16}$$

M_{sp}, M_{rf}, M_v are moments due to spring, roller inertia and valve. These moments and their associated forces are given by the following equations.

$$M_{sp} = F_{sp}B \cos\left(\frac{\pi}{2} - \gamma - \chi\right) \tag{17}$$

$$M_{rf} = f_{rf}B^2 \tag{18}$$

$$M_v = F_v B \cos\left(\frac{\pi}{2} - \gamma - \chi\right) \tag{19}$$

$$F_{sp} = k(l_v + \delta) \tag{20}$$

$$f_{rf} = M_f \omega^2 \frac{d^2\gamma}{d\phi^2} \tag{21}$$

$$F_v = M\omega^2 \frac{d^2 l_v}{d\phi^2} \tag{22}$$

δ is pre-compression in valve spring which is required to close the valve during the dwell period.

2.3   Contact Geometry

Dimensions of contact area and maximum pressure distribution are calculated by referring to the theory of elastic contact for cylinders developed by Hertz [17]. The contact parameters are given by the following equations. The maximum pressure is given by:

The maximum pressure is given by

$$P_{max} = \left(\frac{2W}{\pi l b}\right) \tag{23}$$

where b half-width of Hertzian contact

$$b = \sqrt{\frac{8WR_e}{\pi l E'}} \tag{24}$$

Semi elliptical pressure distribution is defined as

$$P = P_{max}\sqrt{\left(1 - \frac{x^2}{b^2}\right)} \tag{25}$$

The contact area now can be defined as

$$A_a = 4lb \tag{26}$$

The equivalent radius of curvature R_e and equivalent elastic modulus E' are given as

$$\frac{1}{R_e} = \frac{1}{R} + \frac{1}{r_R} \tag{27}$$

$$\frac{2}{E'} = \frac{1-v_1^2}{E_1} + \frac{1-v_2^2}{E_2} \tag{28}$$

2.4   Lubrication Analysis

The cam/roller pair operates under severe conditions and oil film thickness (OFT) is influenced by several parameters like entrainment velocity, flash temperature and contact loading. The lubrication at cam/roller interface varies all the way from elastohydrodynamic to mixed lubrication. The minimum and central lubricant film thickness can be predicted by the relation provided by Dowson and Higginson [18] and Dowson and Toyoda [19], respectively.

$$\frac{h_m}{R} = 2.65\ U^{.70}\ G^{.54}\ W'^{-.13} \tag{29}$$

$$\frac{h_c}{R} = 3.06\ U^{.69}\ G^{.56}\ W'^{-.10} \tag{30}$$

The dimensionless film thickness parameter serves as a basis for the classification of lubrication regimes. The dimensionless film thickness greater than one corresponds to elastohydrodynamic lubrication, for value of $0 < H < 1$, the contact operates in mixed lubrication regime and value of H approximately reaches to zero when boundary lubrication is

in action and coefficient of friction no more depend on lubricant viscosity, entrainment velocity, load and the contact area.

$$H = \frac{h_m}{\sigma}$$

(31)

σ is composite surface roughness given as:

$$\sigma = \sqrt{\sigma_1{}^2 + \sigma_2{}^2}$$

(32)

2.5 Friction Model

Three types of friction forces play their role in determining the frictional torque at cam/roller interface i.e. hydrodynamic, rolling and boundary friction force. Hydrodynamic friction becomes prominent in regions of high roller slip especially at cam flanks due to high sliding velocity. Hydrodynamic friction force can be predicted in the proximity of Hertzian contact by the following relation.

$$F_h = \int_{-b}^{+b} \frac{2n_p V_s l}{h_{cen}} dx$$

(33)

In order to determine the viscosity of lubricant at elevated pressure, Chu and Cameron [20] relation has been used since the pressure ranges up to 0.64 GPa which is well within the pressure range of 1 GPa specified in work. The simple Baraus equation cannot work in the present work due to the limitation of its maximum operating pressure range of 0.1 GPa. In the presented study, even after meeting the upper value of pressure constraint for Chu and Cameron equation, it overpredicts the viscosity at high pressure, therefore, a limiting friction coefficient of value 0.08 has been adopted. In case, the elastohydrodynamic coefficient of friction exceeds the limiting value, the hydrodynamic friction is determined by $F = 0.08W$. OFT at the cam nose region may not be enough to ensure the complete separation of mating surfaces of cam

and roller. When the OFT have values lower than the composite surface roughness height, mixed to boundary lubrication regime can exist at this region [20-21] and load is partially taken by the asperities in the contact region which can be calculated by Greenwood and Trip model [21].

$$W_a = \frac{8\sqrt{2}}{15} \pi (\beta \sigma \eta)^2 E' \left(\frac{h}{\sigma}\right) A \, F_{\frac{5}{2}} \sqrt{\frac{\sigma}{\beta}} \tag{34}$$

The values of 0.04 and 0.01 are chosen for $(\beta \sigma \eta)$ and $(\frac{\sigma}{\beta})$ respectively based upon the recommendation of Greenwood and Trip in their study. The asperity contact area is given as.

$$A_r = \pi^2 (\eta \beta \sigma) A \, F_2 \left(\frac{h}{\sigma}\right) \tag{35}$$

Asperity height distribution is given by the following relation

$$F_n(H) = \frac{1}{\sqrt{2\pi}} \int_H^\infty (s - H)^n \, e^{-\frac{s^2}{2}} ds \tag{36}$$

The hydrodynamic pressure developed in lubricant film under the action of the load is determined by[22].

$$P_H = \frac{W - W_a}{A_a - A_r} \tag{37}$$

Boundary friction force acting due to the resistance of the thin surface film is given by the following relation

$$F_b = \tau_0 A_r + \mu_B W_a \tag{38}$$

Finally, the rolling friction force can be determined by [23].

$$F_r = \frac{4.318(GU)^{0.658} W^{0.0126} 2lR}{\alpha} \tag{39}$$

Total friction force and coefficient of friction for end pivoted finger roller follower can be predicted as follows

$$F = F_b + \left(1 - \frac{A_r}{A_a}\right) F_h + F_r \tag{40}$$

$$\mu = \frac{F}{W} \tag{41}$$

Cam roller friction torque can be obtained by multiplying cam roller total friction force with the normal distance from cam center to point of action of friction force at cam surface.

2.6. Cam Bearing Friction Model

Schematic of understudy camshaft is shown in Fig.3. The cam bearing hydrodynamic friction can be predicted by assuming the full film lubrication with Newtonian lubricant. Crane previous work [24] also supports the assumption of considering only hydrodynamic conditions for cam bearing frictional even at low camshaft speeds.
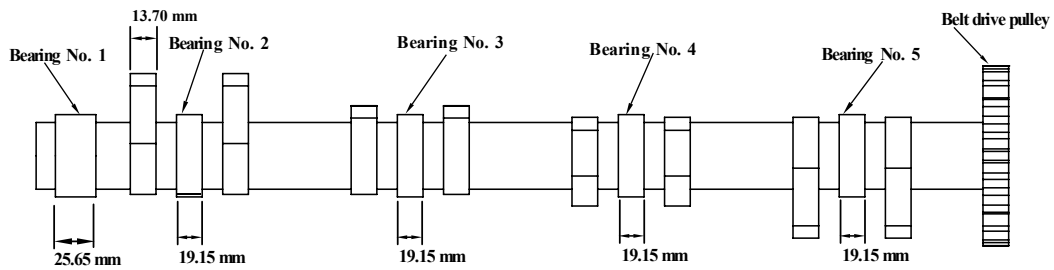
Fig. 3. Schematic of camshaft

$$S = \frac{(2+n^2)(\sqrt{1-n^2})}{12\pi^2 n}$$

(42)

"n" is the eccentricity of bearing and "S" is Sommerfeld number.

$$S = \frac{\eta_0 \omega L_B D_b}{W_B} \left(\frac{D_B}{2c}\right)^2 \tag{43}$$

W_B is instantaneous load on bearing which is due to reaction and friction force at the cam roller interface. The bearing load is calculated by assuming the camshaft composed of rigid beams in series and forces are only due to immediate cams. Bearing loads are then calculated by setting up a static balance for each rigid beam with cam load. Frictional force for each cam bearing is calculated by the following equation.

$$F_B = \frac{2r^2 \eta_0 L_B \omega}{12c} \frac{4\pi^2(1+2n^2)}{(2+n^2)(\sqrt{1-n^2})} \tag{44}$$

2.8. Valve/guide & Needle roller bearing Friction

Although the friction contributed by valve guide interface has a negligible effect on overall friction of valve train but it has been addressed for the completeness of model. The hydrodynamic friction force for fully lubricated Couette flow in valve guide with the assumption of concentric valve moment in the radial clearance of valve stem and valve guide is given as [25].

$$F_{vg} = \eta_0 \frac{V_v}{C_v} \pi d_v L_v \tag{45}$$

V_v is valve velocity which can be obtained by numerically differentiating lift data.

The needle roller bearing is assumed to operate in boundary lubrication regime. Kubiak et al. [26] use the following relation to calculate the friction of the needle roller bearing frictional torque in rocker arm of roller follower valve train.

$$F_{NB} = \mu_p W r_p \tag{46}$$

Where μ_p is the roller needle bearing coefficient of friction and r_p is the radius of the needle roller pitch circle. Flow chart for the calculation of drive torque including the effects of roller sliding and asperity interaction is shown in Fig. 4.
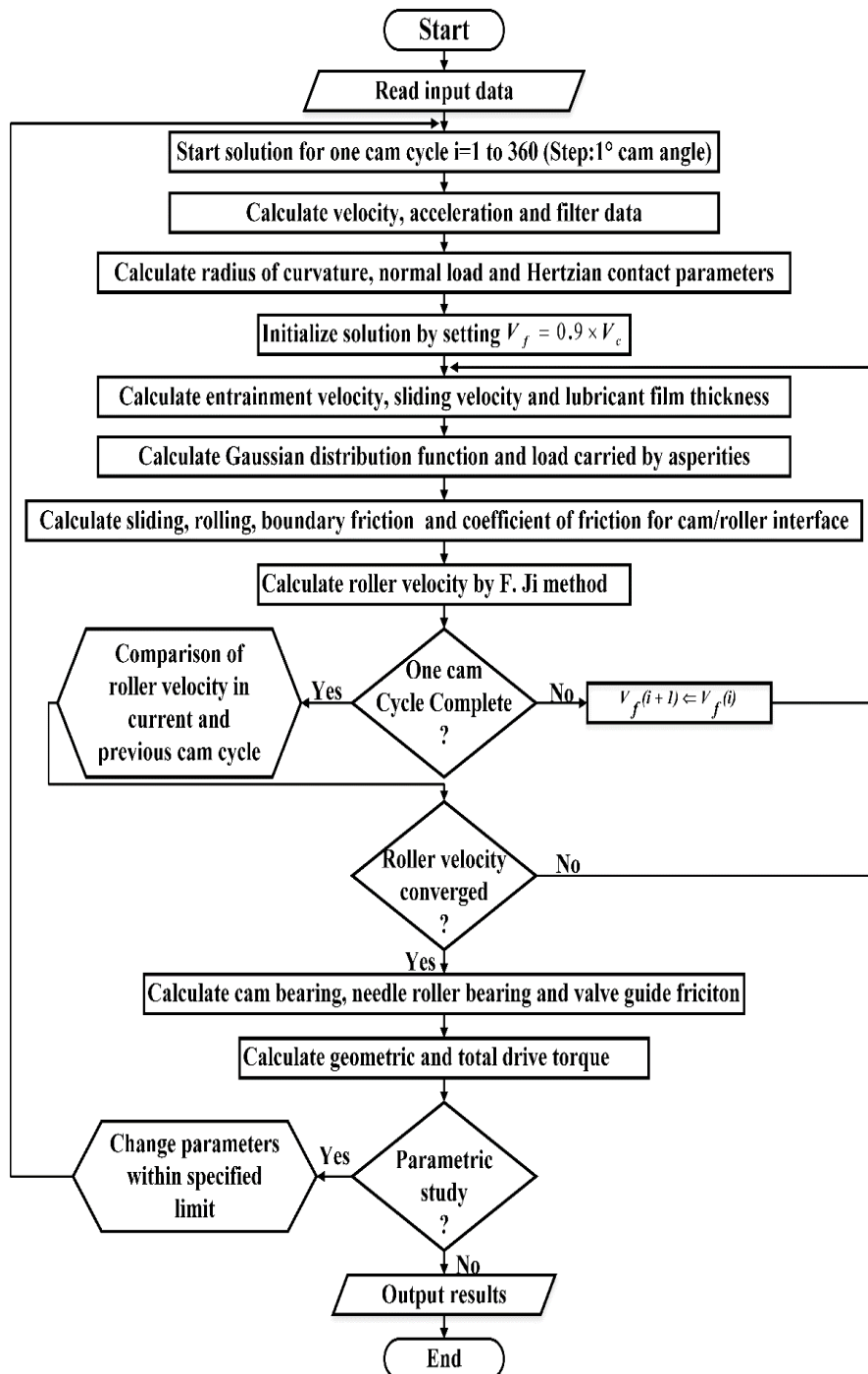
Fig. 4. Flow chart for friction modeling of end pivoted finger roller follower valve train

CHAPTER 3: RESULTS AND DISCUSSION

The simulations have been carried out at three different camshaft rotational frequencies 300 RPM, 600 RPM and 900 RPM and three different lubricant bulk temperatures 25°C, 60°C and 95°C to mimic the actual engine operating conditions. A detailed parametric study has been undertaken under different operating conditions. The summation of frictional forces due to cam/roller contact, needle roller bearing, valve/guide friction and cam bearing friction is presented in the form of drive torque.

The frictional characteristic at cam/roller contact is governed by the contact loading, significantly. The plot of normal loading at the cam/roller interface at different camshaft rotational frequency is shown in Fig. 5. At lower RPM, the profile is dominated by the spring load which acts mainly at cam nose position. The magnitude of contact loading increases in the cam flank region as the inertia of reciprocating masses come into play at higher cam speeds.
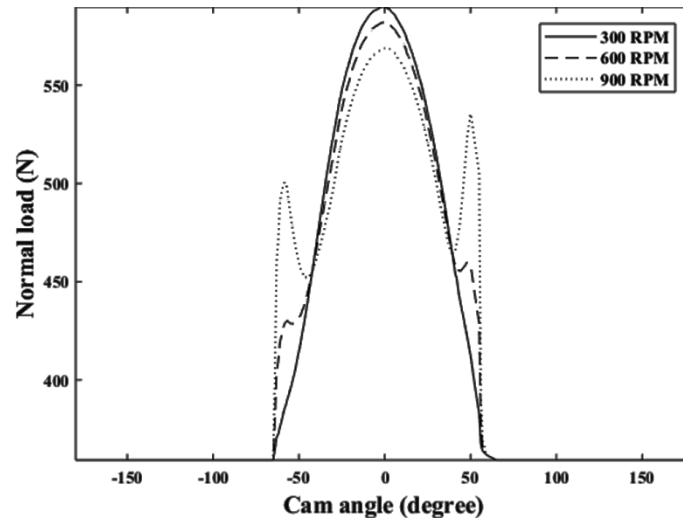
Fig. 5. Cam/roller contact loading profile

Entrainment velocity of lubricant is high at cam flank regions which decrease rapidly at cam nose region. An increasing trend in entrainment velocity by increasing cam speed is evident.
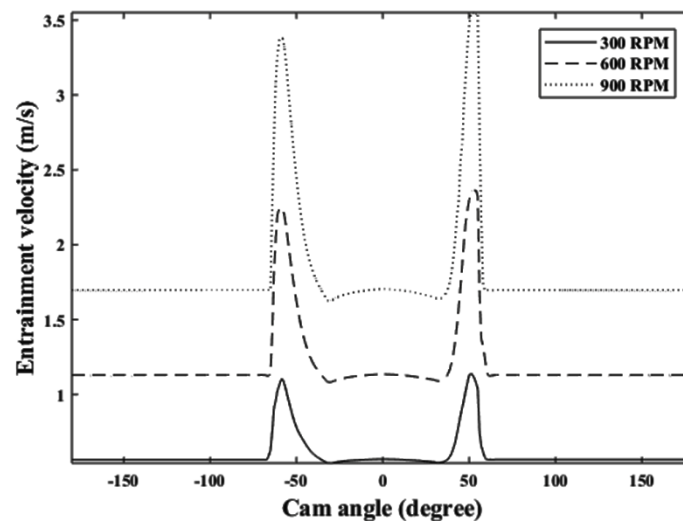
Fig. 6. Entrainment velocity

OFT Plot at cam/roller junction is shown in Fig. 7. Since the entrainment velocity controls the amount of oil driven in the contact region, therefore, the OFT follows its trend accordingly. At high camshaft rotational frequency, flanks enjoy healthy film thickness as compared to the nose region though the contact load is high at flanks. Healthy film thickness at cam flank indicates that the hydrodynamic friction is dominant at that region. The poor lubrication condition at the nose region increases the asperity interaction and the contact tends to operate in boundary lubrication regime. Increase in the magnitude of OFT is predicted by increasing camshaft rotational frequency due to rise in entrainment velocity. The OFT being the function of lubricant bulk viscosity decreases with increasing oil supply temperature.
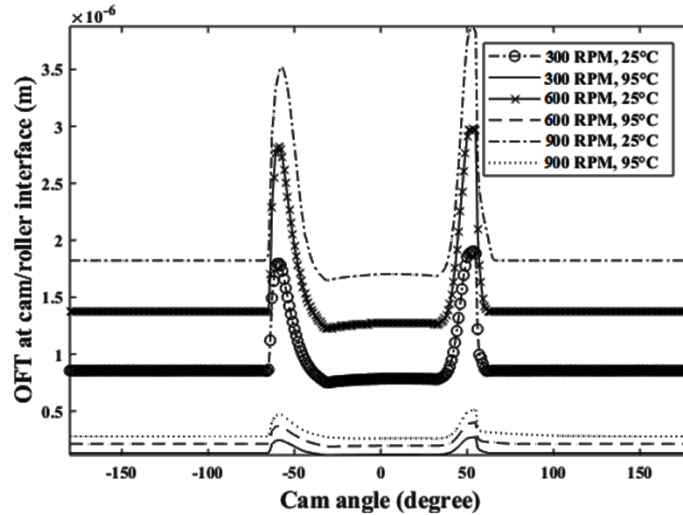
Fig. 7. Oil film thickness at cam/roller interface

Total friction at cam/roller interface is dominated by sliding friction, especially at low lubricant supply temperature. Sliding friction is mainly affected by two factors the sliding velocity and lubricant viscosity at elevated pressure. Lubricant viscosity at elevated pressure is affected by hydrodynamic pressure as defined in Eq. (25) and viscosity profile at increased pressure is similar to hydrodynamic pressure profile which is greatly influenced by the normal load at cam/roller interface.

At lubricant bulk temperature of 25°C, there is an increasing trend in the cam/roller interface friction force by increasing the camshaft rotational frequency as shown in Fig.8. The major portion of cam/roller interface friction is due to sliding friction arising due to shearing of lubricant and is strongly influenced by the sliding velocity as defined in Eq. (8). A healthy oil film is formed at low operating temperature and overall behavior of friction force is dominated by the hydrodynamic friction force. By increasing the camshaft rotational frequency, the roller slip at flank regions arises due to the roller inertia and thus the sliding friction also becomes dominant at flank regions. Moreover, the flank region enjoys a thicker film thickness than other cam regions resulting in the high magnitude of hydrodynamic friction and relatively more power is lost in shearing of a relatively thick film.

16
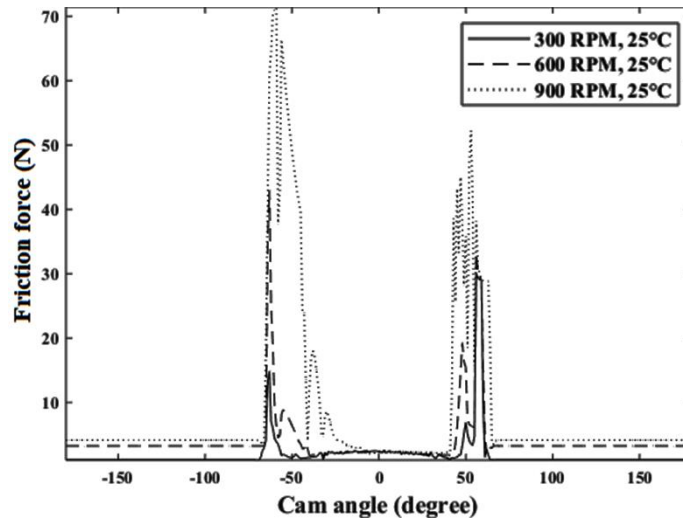
Fig. 8. Cam/roller interface friction force at 25°C and different cam speeds

In Fig. 9, at low lubricant supply temperature, the percentage of asperity friction is almost negligible. It can also be seen that at cam angles from 116° to 137° and 222° to 242°, there is almost no contribution of boundary friction to the total cam/roller friction, as this area corresponds to cam flank region which enjoys relatively a greater film thickness. The percentage of asperity friction to total friction at cam/roller interface shows a decreasing trend by increasing the cam rotational frequency which is attributed to the rise in film thickness.
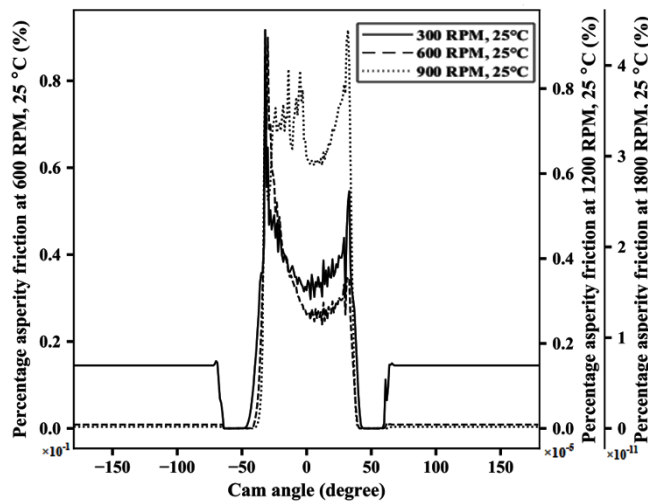
Fig. 9. Percentage asperity friction at 25°C and different cam speeds

By increasing the lubricant supply temperature to 60°C, a noticeable decrease in the sliding friction occurs which reduces the cam/roller interface friction considerably as shown in Fig.10. Although there is an increase in boundary friction due to rise in asperity interaction by increasing the temperature. The total friction at the cam/roller interface decreases by increasing oil supply temperature from 25 °C to 60 °C. By increasing camshaft rotational frequency, a considerable rise in cam/roller friction is also evident at flanks due to the increase in contact loading and roller sliding. However, at cam nose region, almost negligible change is observed as compared to the cam flanks.
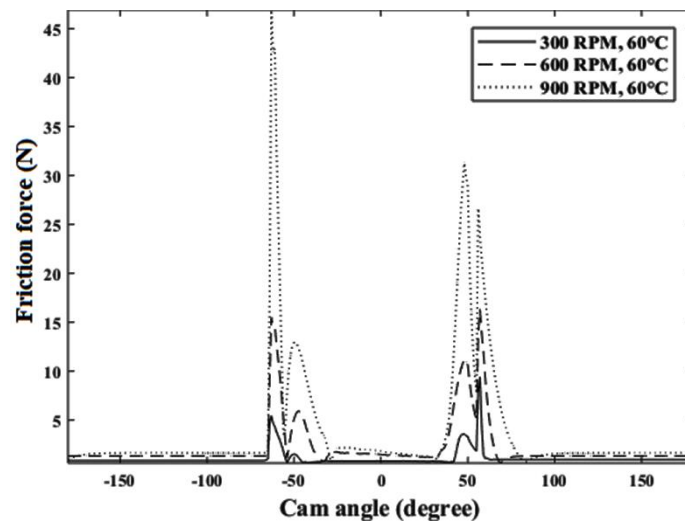
Fig. 10. Cam/roller interface friction force at 60°C and different cam speeds

By increasing the lubricant supply temperature to 60°C, the effects of asperity friction become significant which were nearly negligible at 25°C. This also highlights the importance of inclusion of asperity friction while predicting the cam/roller interface friction. The percentage of asperity friction at cam speed of 300 RPM and oil temperature of 60°C rose up to 60% at cam nose region as compared to oil temperature of 25°C while operating at the same cam speed due to poor lubrication conditions as shown in Fig.11. By increasing the cam speed, a noticeable reduction in percentage contribution of boundary friction is also observed due to the rise in OFT.
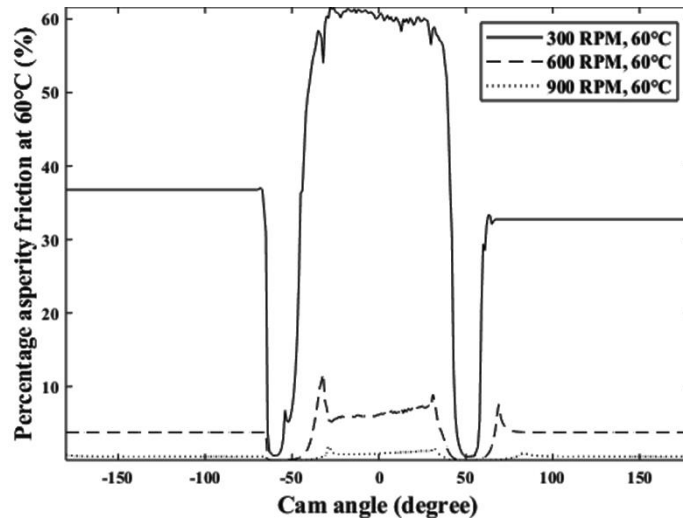
Fig. 11. Percentage asperity friction at 60°C and different cam speeds

At low camshaft, rotational frequency and high oil supply temperature of 95°C, relatively less oil is driven into the cam/roller contact zone. The cam/roller contact friction has the substantial contribution of the boundary friction which is prominent in the cam nose region as shown in Fig.12. By increasing the camshaft rotational frequency, there is an increase in the cam/roller interface friction force due to the rise in roller slip and normal load at the flank region. The increased roller slip is responsible for the rise in sliding velocity as given in the Eq. (8). The increase in roller slip by increasing the camshaft rotational frequency has also been experimentally proven by Khurram et al. [10]. While the gradual decrease in cam/roller interface friction at cam nose region is due to decrease in inertial load at cam nose region by increasing camshaft rotational frequency from 300 RPM to 900 RPM. The cam/roller interface friction at 95°C decreased by increasing the camshaft rotational frequency from 300 RPM to 600 RPM. By further increasing the camshaft rotational frequency from 600 RPM to 900 RPM, the increase in sliding friction is dominant than the reduction in the boundary friction and the average value of cam/roller friction is more at 900 RPM as compared to 600 RPM.
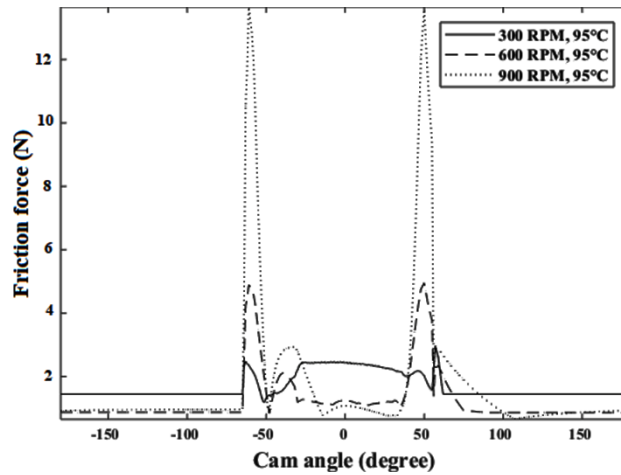
Fig. 12. Cam/roller interface friction force at 95°C and different cam speeds

By increasing the oil supply temperature from 60°C to 95°C, the percentage asperity friction has increased about 82% at 300 RPM which further predicts a downward trend by increasing the cam speed due to improved lubrication and reduced contact load at cam nose region.
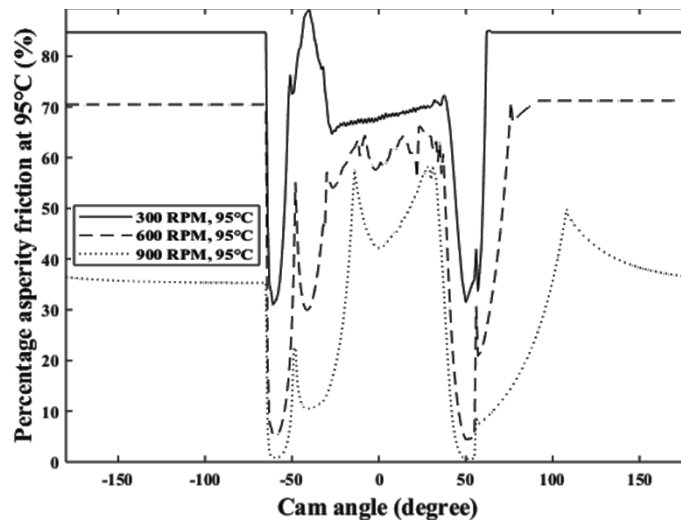
Fig. 13. Percentage asperity friction at 95°C and different cam speeds

By comparing the results for percentage asperity friction at all oil supply temperature and camshaft rotational frequency, it is evident that asperity interaction is dominant at lower camshaft frequency due to higher contact loading at cam nose region and poor lubrication conditions due to low entrainment velocity. By increasing the oil supply temperature, the

asperity interaction increases and contact operating condition shifts towards boundary lubrication due to decrease in OFT
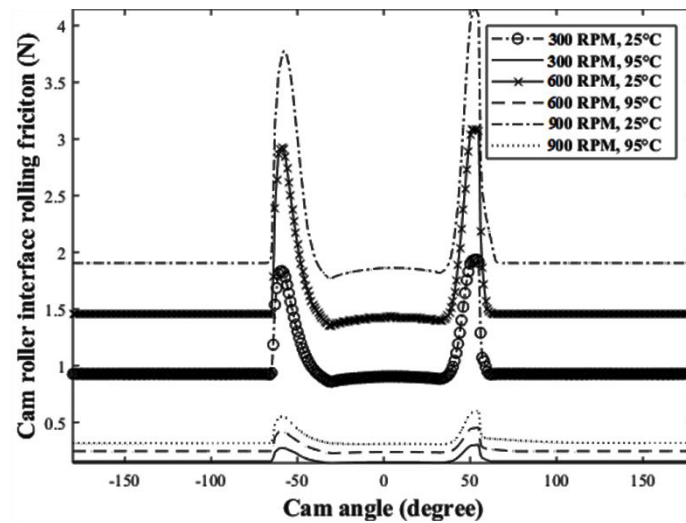
Fig. 14. Rolling friction at cam/roller contact

The third component that contributes to the cam/roller interface friction is rolling friction which shows an increasing trend by increasing camshaft RPM having a maximum value at 900 RPM and 25°C. The magnitude of rolling friction decreases with increasing inlet oil temperature having the lowest contribution in total cam/roller interface friction at 300 RPM and 95°C condition.

After calculating the total friction at cam/roller contact the F Ji [8] model was used to calculate the roller slip at cam/roller contact which gives rise to higher magnitude of hydrodynamic friction force which was neglected before when pure rolling conditions were assumed.

The predicted instantaneous roller slip ratio for one cam revolution at camshaft rotational frequency of 300, 600 and 900 RPM and at different oil supply temperatures are shown in the following figures. The roller slip is very significant at flanks regions and small amount of slip also present at base circle while in cam nose area there is the almost pure rolling

condition, especially at lower RPM. Due to intrinsic nature of roller slip there is an increase in sliding friction as roller slip increases and this increase in friction tries to bring the roller surface velocity to be in line with cam surface velocity, therefore, the areas of high roller slip ratio are immediately followed up by the areas of very low roller slip ratio. At low camshaft rotational frequency the value of roller slip observed is less than 600 and 900 RPM also the friction force in needle roller bearing and inertia of the roller is not very significant at this speed relative to higher RPM. There is an increasing trend in roller slip ratio by increasing camshaft rotational speed due to higher operating conditions and roller inertia would play an important role at higher RPM. At 600 and 900 RPM reduction in contact load at cam nose area due to the increased tendency of roller acceleration being negative at the nose by increasing camshaft speed and reduced asperity interaction due to healthier OFT there is an increase in roller slip ratio at cam nose region by increasing cam speed. The negative slip at flank regions is because of roller surface velocity is unable to follow the rapid fall/increase in cam surface velocity instantly due to roller inertia and roller surface velocity is more than cam surface velocity at that instant. By increasing oil supply temperature there is an increase in roller slip ratio due to decrease in hydrodynamic viscous shearing force at elevated temperature and as sliding force is at the top of the list in the hierarchy of friction force at cam/roller interface, therefore, a decrease in sliding friction decreases the overall friction force and accordingly by slip model commissioned in numerical model predicts an increase in roller slip by increasing oi supply temperature.
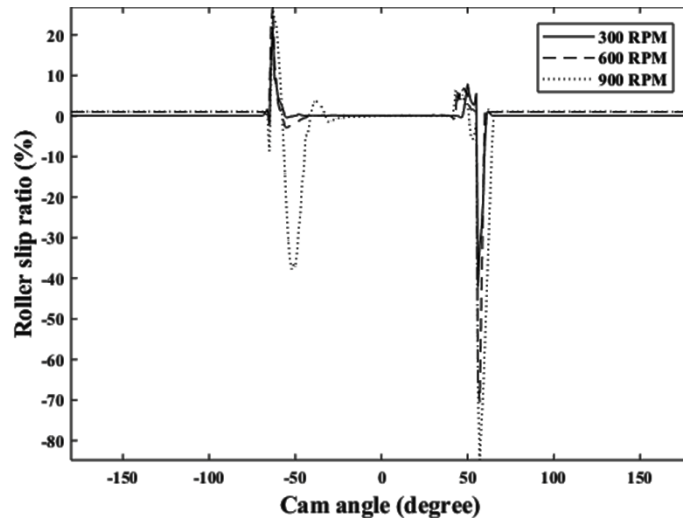
Fig. 15. Roller slip ratio at oil supply temperature of 25°C

Fig. 16 presents roller slip ratio at oil supply temperature of 60°C a significant decrease in roller slip is observed at flanks regions while the nose area being operated in boundary lubrication regime all the time has no changes.
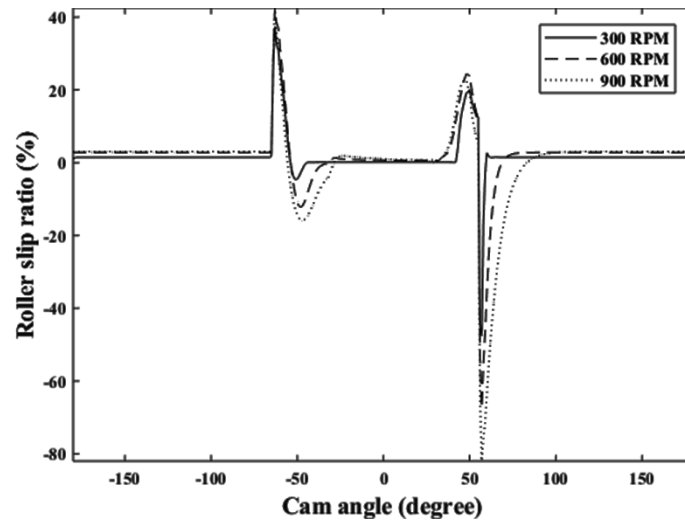
Fig. 16. Roller slip ratio at oil supply temperature of 60°C

By further increasing oil supply temperature from 60 °C to 95 °C again a little drop in roller slip ratio at flank regions is observed while the effects of camshaft rotational frequency are consistent at all temperatures. Moreover, at higher temperature of 95 °C the friction force at cam/roller interface is significantly less than at 25 °C and 60 °C and effects of inertia are relative more dominant than at lower temperatures where friction force is relatively high so

the variation in roller surface velocity from cam surface velocity not very rapid as inertia makes it difficult for roller to change its speed abruptly.
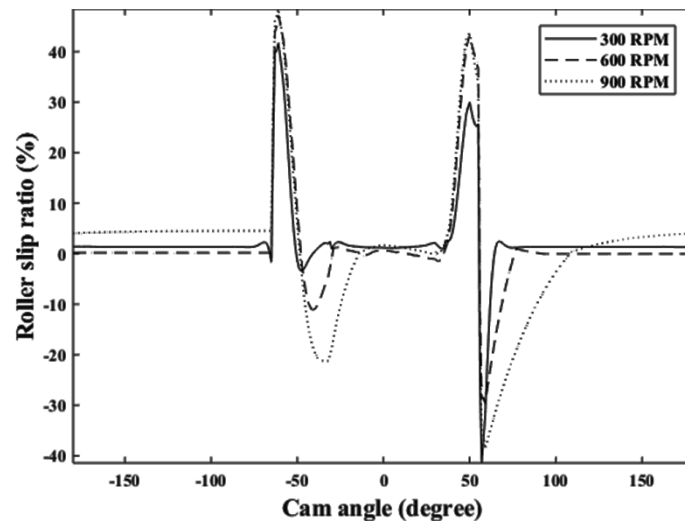
Fig. 17. Roller slip ratio at oil supply temperature of 95°C

The average roller slip ratio at different operating conditions is presented in Fig. 18. The rise in roller slip ratio by increasing camshaft rotational frequency can be observed and the magnitude of roller slip ratio by changing camshaft rotational speed is comparable with the experimental findings of Khurram et al. [10]. However, the variation in roller slip w.r.t oil supply temperature is contradictory to that of author mentioned before this is because model predicts thee lubrication regime to be mostly in hydrodynamic regime and a decrease in friction force by gradually increasing oil supply temperature leads to increased roller slip.
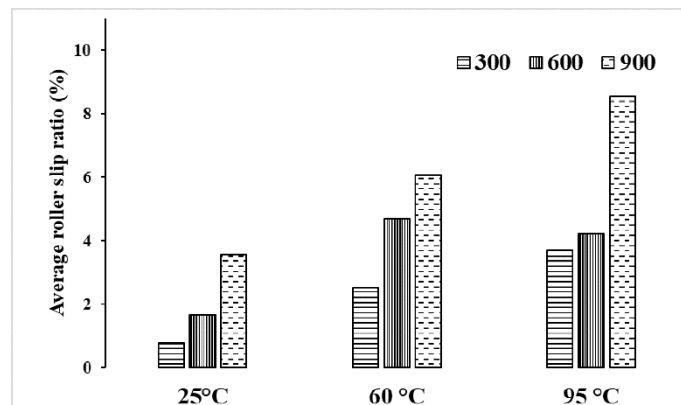
Fig. 18. Average roller slip ratio at different operating conditions

Average values of frictional torques for one complete revolution of the camshaft are given in Fig. 19. There is an increase in the average value of frictional torque w.r.t camshaft rotational frequency. The decrease in the average value of friction by increasing the temperature shows that the model also caters for the viscous effects of lubricant particularly at higher RPM when effects of sliding friction are dominant due to the roller sliding. Moreover, this decrease in average value w.r.t temperature may be due to a fixed value of limiting friction coefficient used at all operating condition or the journal bearing may be subjected to boundary lubrication condition at some point which is not considered in this study due to qualitative nature of the study. The cam bearing frictional torque arising from the shearing of lubricant under applied load has the largest contribution at 25°C. The highest value of cam bearing friction torque was noticed at 900 RPM and 25°C which is 30% of the total valve train friction torque. Friction torque arising from the valve guide and needle roller bearing is of the same magnitude approximately and accounts for 0.6% to 3% of total valve train friction torque.
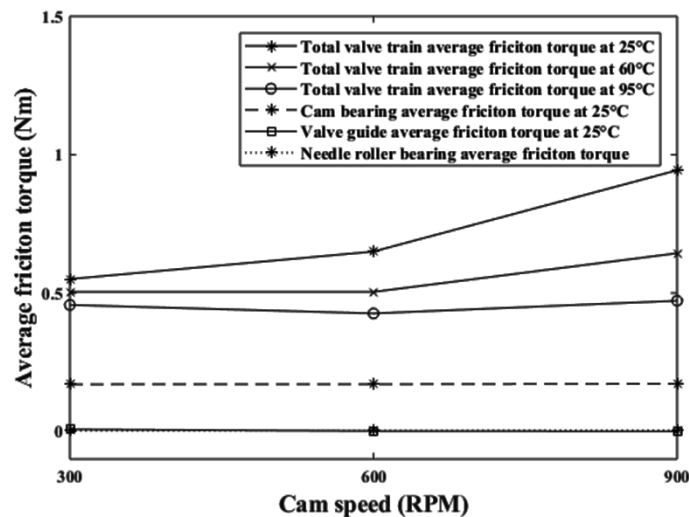
Fig. 19. Average friction torque

25

The incorporation of roller sliding and asperity interaction in the friction modeling for end pivoted roller finger-follower valve train has changed the cam/roller interface friction, significantly as shown in Fig. 15 under different operating conditions. The same highlights the importance of these factors for more accurate prediction of cam/roller interface friction.
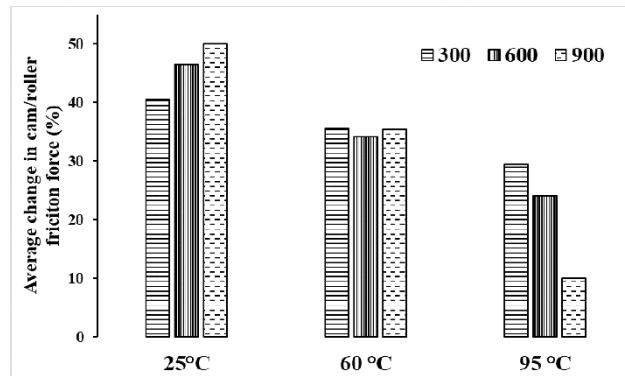
Fig. 20. Average change in cam/roller interface friction force

Fig. 16 present the measured drive torque for end pivoted finger roller follower valve train at three different camshaft rotational frequencies of 300, 600 and 900 RPM at lubricant supply temperatures 25°C, 60°C and 95°C. One thing to be kept in mind is that experimental drive torque composed of geometric torque experienced due to the work of cam against spring load while opening and closing of the valve and frictional torque which is the sum of the frictional torque contributed from cam/roller contact, cam bearing, valve guide and needle roller bearing. The variation in drive torque is only because of change in magnitude of frictional force as geometric torque is merely affected by change in engine speed and has absolutely no effect of change in oil supply temperature.

(a)

(b)

(c)

(d)

(e)

(f)

27
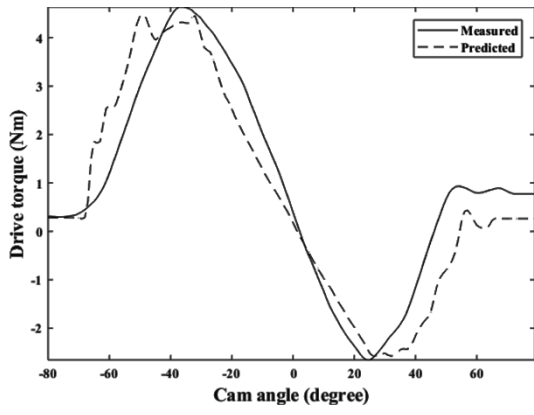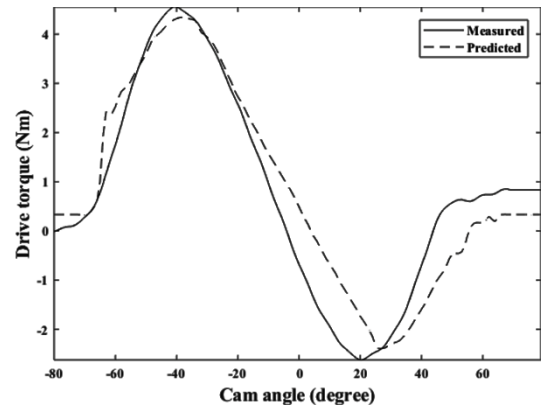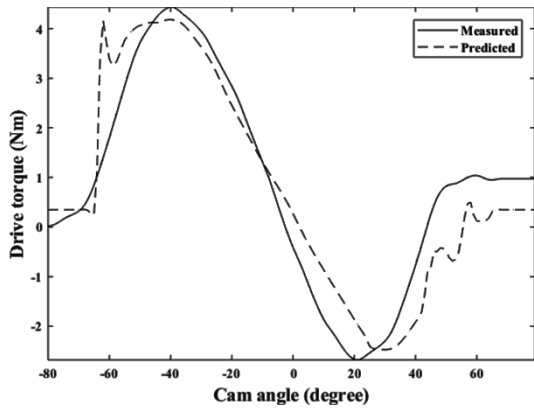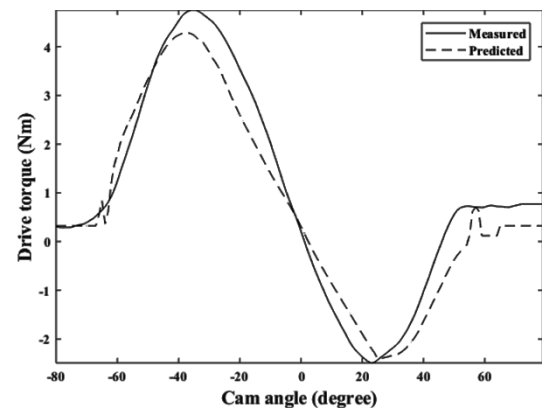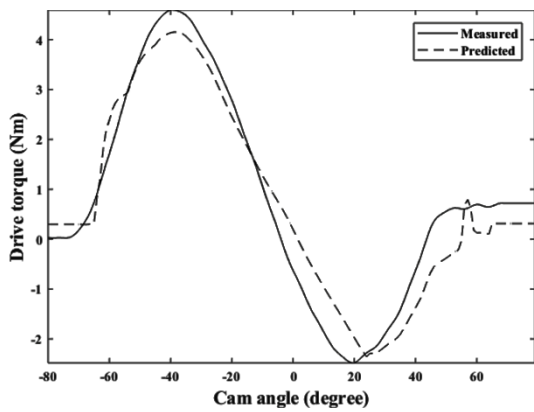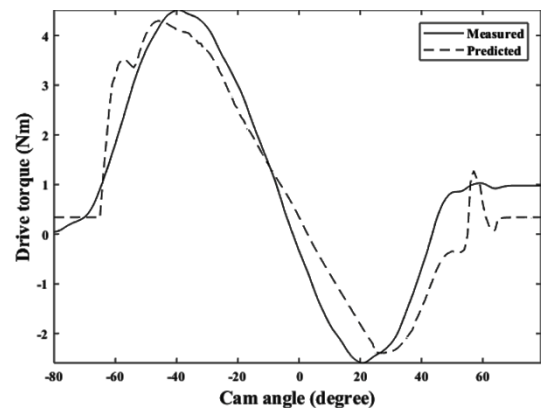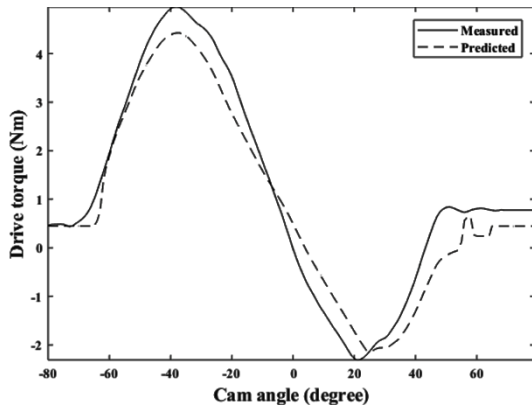
(g)
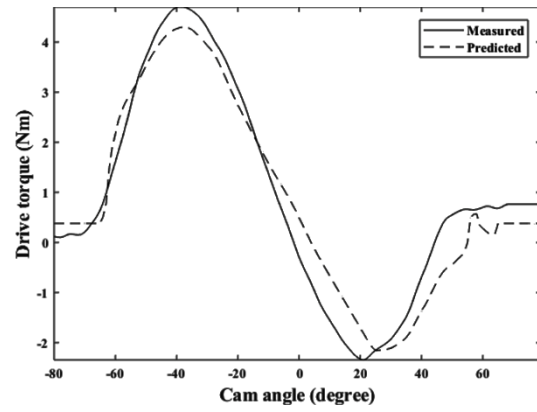
(h)
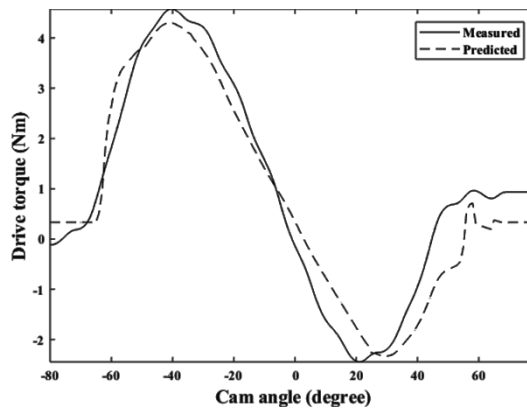
(i)

Fig. 21. Comparison of instantaneous measured and predicted drive torque (a) 300 RPM, 25°C (b) 600 RPM, 25°C (c) 900 RPM, 25C (d) 300 RPM, 60°C (e) 600 RPM, 60°C (f) 900 RPM, 60°C (g) 300 RPM 95°C (h) 600 RPM 95°C

In above Figures it can be observed that there is a decrease in the drive torque by increasing camshaft rotational frequency this attribute is due to improved lubrication condition as high entrainment velocity drive more oil in to the highly pressurized contact zone and a healthier oil film thickness shifts the lubrication regime towards hydrodynamic lubrication which sure there is less metal to metal contact resulting in improved overall tribological performance. Moreover, at low RPM the contact loading on cam/roller contact is greatly influenced by spring loading which is more dominant at the cam nose region as the RPM increases the effect of the inertial load become more dominant and loading becomes more concentrated at flanks region. Thus, by increasing camshaft rotational frequency the cam/roller

28

contact experience reduces pressure especially at cam nose area which reduces the friction force.

An increase in drive torque by increasing oil supply temperature is evident. This phenomenon is due to the poor lubrication condition arises as the thin oil film thickness is present at the cam/roller interface. By increasing the oil supply temperature, the effect of surface roughness at cam/roller contact came into action as oil film thickness becomes thin the asperity interaction increases which forces the lubrication regime towards mixed to absolute boundary lubrication where there are more chances for metal to metal contact.

The comparison of predicted and measured drive torque for the cam action period is presented in Fig. 16. The predicted drive torque is composed of two components one is frictional torque that arises from the friction forces from cam/roller contact, needle roller bearing, valve guide and cam bearings friction other is geometric torque that which is due to the opening and closing of the valve against the spring force. The geometric torque, having equal positive and negative parts, is taken as positive during the opening of the valve and negative during the closing of the valve. Upon the addition of predicted geometric and frictional torque as frictional torque is positive for entire cam cycle the positive part of the geometric torque increases and negative part reduces as upon addition frictional torque makes it less negative.

There is fine conformity between predicted and experimental instantaneous drive torque although during valve closing the predicted drive torque slightly underpredicts than measured values this behavior may be due to the minute leakage of oil from hydraulic lash adjuster that can disturb the compression of spring and geometric torque is not fully recovered during valve closing. This cumbersome phenomenon of un-symmetric drive torque shape around the cam nose must be kept in mind while analyzing the results.

The comparison of average values of predicted and measured frictional torque is presented in Fig. 17. As geometric torque has equal positive and negative parts thus by taking average its effect can be diminished and only average frictional torque can be obtained in case of measured data.

The predicted friction torque includes friction from cam/roller contact, cam bearings, valve guide and needle roller bearing. There is a decrease in average fiction torque for camshaft rotational frequency of 300 and 600 RPM when oil supply temperature is increased from 25 °C to 60 °C and then an increase from 60 °C to 95 °C depicting a decrease in hydrodynamic friction followed by an increase in boundary friction due to increased asperity interaction at elevated temperature. However at 900 RPM a gradual decrease in predicted average frictional torque by increasing oil supply temperature from 25 °C to 95 °C can be observed this attribute arises due to the relatively high contribution of cam bearing friction as it increases by increasing camshaft rotational speed and shows a downward trend by increasing temperature as less resistance is faced by cam journal bearings in the shearing of a less viscous oil.
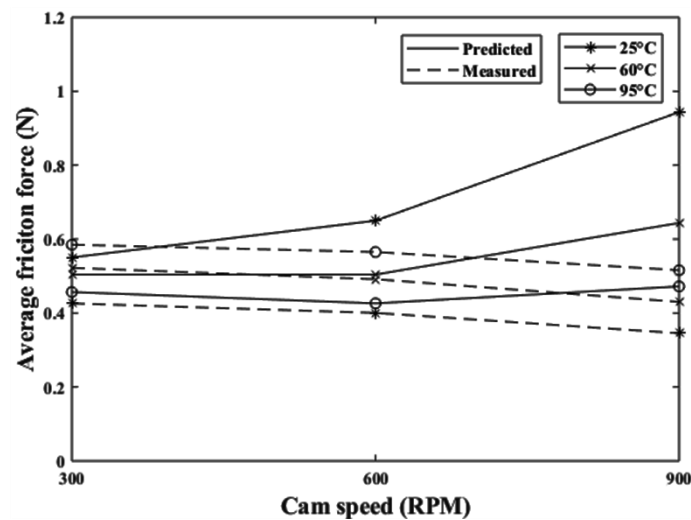
Fig. 22. Comparison of average predicted and measured friction force

Overall a reasonable agreement between predicted and measured results is noticed. The model is also able to predict the trend of experimental data to some extent which is very encouraging for such a complex mechanical system. This study finds it worth as one purpose

30

of this study is to validate the frictional model described in this paper which can provide

footsteps for future modeling in this specific research area.

CHAPTER 4: THESIS CONCLUSION & RECOMENDATION

4.1 Conclusion

A detailed mathematical model has been developed by considering the roller sliding, asperities interactions at the mating surfaces of cam and roller and contributions from bearings, valve/guide interface and roller needle bearings. The friction in end pivoted roller finger-follower valve train has been evaluated successfully considering the effects of different camshaft rotational frequency and lubricant supply temperature.

It has been found that the sliding friction at cam/roller contact is a major contributor to the total valve train friction due to sliding of the roller, especially at cam flanks region. Sliding friction showed a rising trend by increasing the camshaft rotational frequency which reduced greatly at higher oil supply temperatures. The asperity friction is highly dependent on the oil film thickness which reduces by increasing the cam rotational frequency due to better entraining velocity. The contribution of asperity friction is almost negligible at lower temperature but becomes significant at higher oil supply temperature. It is also evident that consideration of asperity interaction and roller sliding in the friction modeling of roller follower valve train can influence the results, greatly. It is strongly believed that the developed numerical approach can be very helpful to understand the friction in detail thereby allowing to improve the performance of the valve train, significantly.

A numerical approach has been used to validate the result of friction torque. Simulation result includes the friction arising at cam roller contact, valve guide interface and cam bearing friction. The friction arising due to asperity interaction at high lubricant oil supply temperature and roller sliding due to slippage of the roller at cam/roller contact has also been included in model. Overall there is a good agreement between measured and predicted instantaneous drive torque. The average value of predicted drive is also of the same order as measured torque, a

small error is induced may be due to some oil leakage in hydraulic lash adjuster which alter the geometric torque and energy is not conserved during the closing event of valve which has not been addressed and is the limitation of this study. The comprehensive valve train model developed found to be consistent with experimental findings at camshaft rotational frequency of up to 600 RPM however model appeared to be very sensitive to change in operating conditions as compared to experimental data

The comparison of experiments and theory has validated the model and directed future developments of the analysis in relation to the severity of lubrication in both the cam/follower interface and the camshaft bearings, in incorporating the dynamic behavior of hydraulic lash adjusters and consideration of parameters addressing the lubricant chemistry in numerical modeling.

4.2 Suggestions for Future Work

- Model only accounts for lubricant viscosity and the other aspects of lubricant chemistry such as effects of friction modifiers and additives has not yet been accounted till date

- Complete dynamic modeling of valve train system including the damping in valve train components may lead toward further refinement of results

- Numerical model for hydraulic lash adjuster including oil leakage can be integrated with developed model

APPENDIX A

Nomenclature	
A	separation between follower face center of curvature connecting with cam and follower center of rotation.
A_a	apparent area in contact at cam/roller interface
A_r	real area in contact at cam/roller interface
B	separation among the face of roller touching the valve, roller center and its curvature center
b	half-width of Hertzian contact
c	cam journal bearing clearance
D	distance between the center of the roller and cam rotational axis
E	modulus of elasticity
E'	composite elastic modulus, $2/\{[(1 - v_c^2)/E_c] + [(1 - v_f^2)/E_f]\}$
F	total friction
F_b	boundary friction
F_B	cam bearing friction
F_{vg}	valve guide friction
F_{NB}	needle roller bearing friction
F_h	hydrodynamic friction
F_r	rolling friction
F_{sp}	spring force
$F_n(H)$	distribution function (Gaussian)
G	dimensionless parameter for load, $\alpha E'$
H	dimensionless parameter for the thickness of oil film
h_m	minimum thickness of oil film
h_c	central film thickness
l	characteristic half-width
K	spring constant
l_v	valve lift
V_v	valve linear velocity
c_v	radial clearance in valve stem and guide
L_v	valve guide length
d_v	valve stem diameter
W_B	cam bearing load
L_B	cam bearing width
D_B	cam bearing diameter
M	equivalent mass
P	Hertzian pressure
R	equivalent radius of curvature
R_c	cam local radius of curvature
r_B	Cam base circle radius
r_R	roller follower radius
T	temperature (°C)
U	dimensionless speed parameter, $(\eta_o V_{e)})/(E'R)$
V_c	relative velocity of contact point w.r.t cam surface
V_f	relative velocity of contact point w.r.t follower surface
V_s	sliding velocity
V_e	entraining velocity
W	normal load on the contact point

W_a	part of cam load on asperities
W_i	cam base circle load
$\acute{W}$	dimensionless parameter for load, $(W - W_{a)}/(2E'lR)$
α	coefficient used in pressure-viscosity relation
β	asperity radius of curvature
η	asperity density
η_o	ambient pressure dynamic viscosity
η_p	dynamic viscosity at increased pressure
υ	Poisson's ratio
ρ	density
σ_o	composite surface roughness,$\left(\sigma_c{}^2 + \sigma_f{}^2\right)^{1/2}$
μ	friction coefficient
μ_B	boundary friction coefficient
μ_p	friction coefficient used for needle roller bearing
ω	rotational frequency of camshaft
α_r	roller angular acceleration
θ	camshaft angle
λ	constant angle between planes connecting the follower center to the center of curvature of face of follower touching valve and cam
χ	constant angle between valve movement direction and center of rotation of cam and roller
δ	spring pre-compression
γ	variable angle between lines linking follower center to the camshaft center of rotation and the center of curvature of the face of follower touching the valve
ϕ	variable angle between the horizontal axis and the line linking the cam center of rotation with follower
τ	lubricant stress (Eyring)
Subscripts	
c	cam
f	follower
max	maximum
r	roller
b	bearing
v	valve
NB	needle roller bearing

APPENDIX B

Details of Valvetrain:
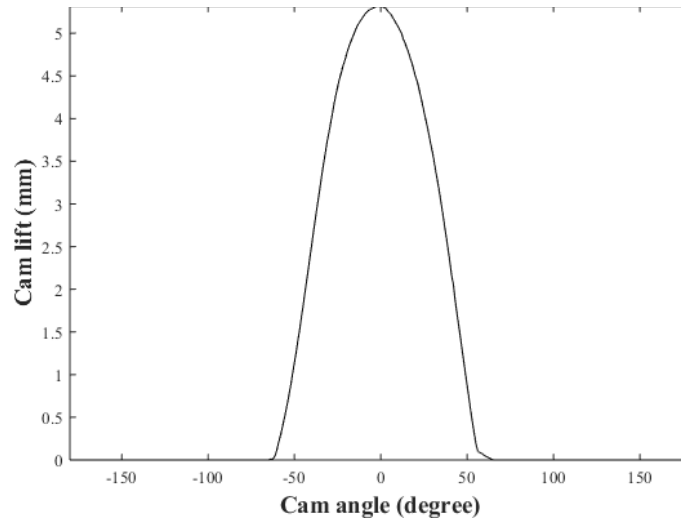
Fig. A. Cam lift profile

Input parameters	
Cam width	0.0137 (m)
Cam Radius	0.018 (m)
Roller diameter	0.017 (m)
Modulus of elasticity of cam	170×10^9 (Pa)
Modulus of elasticity of roller	204×10^9 (Pa)
Cam material Poisson ratio	0.28
Follower material Poisson ratio	0.29
Cam half period action-angle	70 (º)
Spring constant	2500 (N/m)
Pre compression	0.0084 (m)
Roller mass	0.0088 (Kg)
Roller wall thickness	0.0024 (m)
Needle roller radius	0.00099 (m)
Roller finger-follower mass	0.0418 (Kg)
Valve spring and retainer mass	0.0432 (Kg)
Coefficient of friction of needle roller bearing	0.0015
Load on cam Base circle	64 (N)
A	0.02080 (m)
B	0.03550 (m)
D	0.03150 (m)
λ	-3.5 (º)
X	37.5 (º)
Surface roughness	0.14×10^{-6} (m)
Oil grade	SAE 30

Lubricant viscosity at ambient pressure and 25^{0}C	0.15 (Ns/ m^2)
Lubricant viscosity at ambient pressure and 60^{0}C	0.0305 (Ns/ m^2)
Lubricant viscosity at ambient pressure and 95^{0}C	0.01 (Ns/ m^2)
Pressure-viscosity coefficient	0.22×10^{-7}(m^2/N)
Boundary coefficient of friction	0.2
Lubricant Eyring stress	8×10^6 (Pa)
Valve guide length	0.036 (m)
Radial clearance in valve stem and guide	0.002×10^{-3} (m)
Valve stem diameter	0.005 (m)
Clearance in cam journal bearings	0.095×10^{-3} (m)
Cam journal diameter	0.023 (m)

References

[1] Staron J, Willermet PJSt. An analysis of valve train friction in terms of lubrication principles. 1983:625-39.

[2] Schafer F, Van Basshuysen R. Internal combustion engine handbook: basics, components, systems, and perspectives: SAE International; 2004.

[3] Sun D, Rosenberg RJAt. An experimental study of automotive cam-lifter interface friction. 1987;30:167-76.

[4] Colechin M, Stone C, Leonard H. Analysis of roller-follower valve gear. SAE Technical Paper; 1993.

[5] Gecim B. Lubrication and fatigue analysis of a cam and roller follower. Tribology Series: Elsevier; 1989. p. 91-100.

[6] Matthews JA, Sadeghi FJTt. Kinematics and lubrication of camshaft roller follower mechanisms. 1996;39:425-33.

[7] Chiu YJTt. Lubrication and slippage in roller finger follower systems in engine valve trains. 1992;35:261-8.

[8] Ji F, Taylor C. A tribological study of roller follower valve trains. Part 1: a theoretical study with a numerical lubrication model considering possible sliding. Tribology Series: Elsevier; 1998. p. 489-99.

[9] Wang W-z, Wang S, Shi F, Wang Y-c, Chen H-b, Wang H, et al. Simulations and measurements of sliding friction between rough surfaces in point contacts: from EHL to boundary lubrication. 2007;129:495-501.

[10] Khurram M, Mufti RA, Zahid R, Afzal N, Bhutta UJPotIoME, Part J: Journal of Engineering Tribology. Experimental measurement of roller slip in end-pivoted roller follower valve train. 2015;229:1047-55.

[11] Turturro A, Rahmani R, Rahnejat H, Delprete C, Magro LJAPNI-. Assessment of friction for cam-roller follower valve train system subjected to mixed non-Newtonian regime of lubrication. 2012.

[12] Alakhramsing SS, de Rooij M, Schipper DJ, van Drogen MJPotIoME, Part J: Journal of Engineering Tribology. Lubrication and frictional analysis of cam–roller follower mechanisms. 2018;232:347-63.

[13] Abdullah MU, Bhutta MU, Najeeb MH, Khurram M, Mufti RA, Shah SR. Experimental Measurement of Frictional Torque in End Pivoted Roller Finger Follower Valve Train.

[14] Dyson AJTi. Kinematics and wear patterns of cam and finger follower automotive valve gear. 1980;13:121-32.

[15] Lim C, Evans H, Snidle R. Kinematics and lubrication conditions at cam contact in a centrally pivoted cam-finger follower. SAE Technical Paper; 1983.

[16] Ball AD. A tribological study of the design and performance of automotive cams: University of Leeds; 1988.

[17] Hertz HJZRAM. On the contact of elastic solids. 1881;92:156-71.

[18] Dowson D, Higginson GJRM, Mc. Elastohydrodynamic lubrication, 1966. 1983:71.

[19] Dowson D. A central film thickness formula for elastohydrodynamic line contacts, Elastohydrodynamics and related topics. Proc 5th Leeds-Lyon Symp, 1978: Elsevier; 1978.

[20] CHU RYJJI, Petrol. Pressure viscosity characteristics of lubricating oils. 1962;46:147.

[21] Greenwood J, Tripp JJPotiome. The contact of two nominally flat rough surfaces. 1970;185:625-33.

[22] Yang L, Ito A, Negishi H. A valve train friction and lubrication analysis model and its application in a cam/tappet wear study. SAE Technical Paper; 1996.

[23] Goksem P, Hargreaves RJAJLT. The effect of viscous shear heating on both film thickness and rolling traction in an EHL line contact. 1978;100:346-58.

[24] Crane ME, Meyer RCJSt. A process to predict friction in an automotive valve train. 1990:2045-58.

[25] Dowson D, Taylor C, Yang L. Friction modelling for internal combustion engines. Tribology Series: Elsevier; 1996. p. 301-18.

[26] Kubiak P, Siczek KJJoK. The analysis of friction in the bearing of rocker arms. 2016;23.

Tribological Study of Friciton in Roller Follower Valve Train Considering Effects of Asperity Interaction and Roller SLiding

by Tayyab Ul Islam

Tribological Study of Friciton in Roller Follower Valve Train Considering Effects of Asperity Interaction and Roller SLiding

8   Submitted to University of Bradford
    Student Paper   <1%

9   Shivam S Alakhramsing, Matthijn B de Rooij,   <1%
    Mark van Drogen, Dirk J Schipper. "The
    influence of stick–slip transitions in mixed-
    friction predictions of heavily loaded cam–roller
    contacts", Proceedings of the Institution of
    Mechanical Engineers, Part J: Journal of
    Engineering Tribology, 2018
    Publication

10 M Usman Abdullah, Samiur Rahman Shah, M   <1%
    Usman Bhutta, Riaz Ahmad Mufti et al. "Benefits
    of wonder process craft on engine valve train
    performance", Proceedings of the Institution of
    Mechanical Engineers, Part D: Journal of
    Automobile Engineering, 2018
    Publication

11 journals.sagepub.com   <1%
    Internet Source

12 Muhammad Khurram, Riaz Ahmad Mufti, Rehan   <1%
    Zahid, Naqash Afzal, Muhammad Usman
    Bhutta, Mushtaq Khan. "Effect of lubricant
    chemistry on the performance of end pivoted
    roller follower valve train", Tribology
    International, 2016
    Publication

13 R Roshan. "Friction modelling in an engine   <1%
    valve train considering the sensitivity to lubricant
    formulation", Proceedings of the Institution of
    Mechanical Engineers Part J Journal of
    Engineering Tribology, 05/01/2009
    Publication

14 Muhammad Khurram, Riaz A Mufti, Rehan   <1%
    Zahid, Naqash Afzal, Usman Bhutta.

"Experimental measurement of roller slip in end-pivoted roller follower valve train", Proceedings of the Institution of Mechanical Engineers, Part J: Journal of Engineering Tribology, 2015
Publication

15 Y. P. Chiu. "Lubrication and Slippage in Roller Finger Follower Systems in Engine Valve Trains", Tribology Transactions, 2008
Publication   <1%

16 Akemi Ito, Lisheng Yang, Hideo Negishi. "A Study on Cam Wear Mechanism with a Newly Developed Friction Measurement Apparatus", SAE International, 1998
Publication   <1%

17 Submitted to University of Newcastle upon Tyne
Student Paper   <1%

18 C. E. Lim, H. P. Evans, R. W. Snidle. "Kinematics and Lubrication Conditions at Cam Contact in a Centrally Pivoted Cam-Finger Follower", SAE International, 1983
Publication   <1%

19 Muhammad Khurram, Riaz Ahmad Mufti, Muhammad Usman Bhutta, Naqash Afzal et al. "Roller sliding in engine valve train: Effect of oil film thickness considering lubricant composition", Tribology International, 2019
Publication   <1%

20 Submitted to University of Liverpool
Student Paper   <1%

21 M Teodorescu. "Combined multi-body dynamics and experimental investigation for determination of the cam-flat tappet contact condition", Proceedings of the Institution of Mechanical Engineers Part K Journal of Multi-body

Dynamics, 01/01/2004
Publication

22 Khurram, Muhammad, Riaz Ahmad Mufti, Rehan Zahid, Naqash Afzal, Muhammad Usman Bhutta, and Mushtaq Khan. "Effect of lubricant chemistry on the performance of end pivoted roller follower valve train", Tribology International, 2016.
Publication

<1%

23 Bhushan, B.. "Influence of test parameters on the measurement of the coefficient of friction of magnetic tapes", Wear, 19840102
Publication

<1%

24 Xianlin Ouyang, Ho Teng, Xiaochun zeng, Xuwei Luo, Tingjun Hu, Xianlong Huang, Jiankun Luo, Yongli Zhou. "A Comparative Study on Influence of EIVC and LIVC on Fuel Economy of A TGDI Engine Part I: Friction Torques of Intake Cams with Different Profiles and Lifts", SAE International, 2017
Publication

<1%

25 d-nb.info
Internet Source

<1%

26 Kevin Hoag, Brian Dondlinger. "Vehicular Engine Design", Springer Nature, 2016
Publication

<1%

27 F. Ji, C.M. Taylor. "A tribological study of roller follower valve trains. Part 1: A theoretical study with a numerical lubrication model considering possible sliding", Elsevier BV, 1998
Publication

<1%

28 A. Dyson. "Kinematics and wear patterns of cam and finger follower automotive valve gear", Tribology International, 1980
Publication

<1%

29 M. Nadim Ahmed Emira. "Friction-induced oscillations of a slider: Parametric study of some system parameters", Journal of Sound and Vibration, 2007
Publication

<1 %

30 Robert Ian Taylor. "Tribology and energy efficiency: from molecules to lubricated contacts to complete machines", Faraday Discussions, 2012
Publication

<1 %

31 Sheng Li. "Prediction of Spur Gear Mechanical Power Losses Using a Transient Elastohydrodynamic Lubrication Model", Tribology Transactions, 07/2010
Publication

<1 %

32 Shivam S Alakhramsing, Matthijn de Rooij, Dirk Jan Schipper, Mark van Drogen. "Lubrication and frictional analysis of cam–roller follower mechanisms", Proceedings of the Institution of Mechanical Engineers, Part J: Journal of Engineering Tribology, 2017
Publication

<1 %

Exclude quotes	On	Exclude matches	Off
Exclude bibliography	On		